Progress in Engineering Science and Technology
https://engtechprogress.com

Propulsion System Diagnostics for Failure Prevention in Unmanned Aerial Vehicles

Joseph Smith*, Claire C. Morris

Department of Bioresource Engineering, Faculty of Engineering, McGill University, Montreal, Quebec, Canada

Corresponding author: joseph.smith@mcgill.ca

Abstract

The rapid proliferation of unmanned aerial vehicles across civilian, commercial, and military sectors has necessitated unprecedented levels of reliability in their core subsystems. Among these, the propulsion system remains the most critical point of failure, often leading to catastrophic loss of the vehicle and potential collateral damage. This paper presents a comprehensive investigation into predicting failure prevention through advanced diagnostic techniques and experimental analysis of propulsion systems in unmanned aerial vehicles. By shifting the paradigm from reactive failure detection to proactive failure prevention, this research establishes a robust framework for continuous health monitoring. We analyze the degradation signatures of brushless direct current motors and associated aerodynamic components under various stress conditions. Using a custom experimental testbed, we capture multi-modal diagnostic data, including high-frequency vibrational, acoustic, electrical, and thermal signals. Through rigorous analytical processing, we identify precursor anomalies that precede critical component failure. The results demonstrate that specific harmonic distortions in vibration data and transient spikes in current draw serve as highly reliable indicators of impending mechanical and electrical faults. This methodology not only improves the predictive accuracy of maintenance algorithms but also extends the operational lifespan of unmanned aerial vehicles by enabling timely interventions.

Keywords: Failure Prevention; Propulsion System Diagnostics; Unmanned Aerial Vehicles; Experimental Analysis; Predictive Maintenance

1. Introduction

1.1 Context and Motivation

The integration of unmanned aerial vehicles into mainstream logistical, agricultural, and surveillance operations represents one of the most significant technological shifts of the twenty-first century. As these platforms transition from experimental novelties to essential infrastructural tools, the operational demands placed upon them have escalated dramatically. Early applications involved brief, line-of-sight flights in controlled environments, whereas modern deployments often require sustained, autonomous operations in harsh and unpredictable weather conditions [1]. Consequently, the reliability of the underlying mechanical and electronic systems has become a paramount concern for operators, regulators, and manufacturers alike. The propulsion system, typically comprising electronic speed controllers, brushless direct current motors, and aerodynamic propellers, is subjected to immense and continuously varying operational loads. A failure in any single component within this propulsion chain usually results in an immediate and unrecoverable loss of thrust. Unlike multi-engine commercial aircraft that possess substantial redundancy and glide capabilities, the majority of small to medium-sized unmanned aerial vehicles lack the aerodynamic characteristics required to survive a primary propulsion failure. This vulnerability necessitates a fundamental reevaluation of how maintenance and reliability are approached in the unmanned aviation sector [2].

The economic and safety implications of propulsion failures are profound. The loss of an expensive aerial platform and its integrated sensor payload constitutes a significant financial setback. More importantly, as these vehicles increasingly operate in urban and densely populated areas, a propulsion failure poses a severe risk to public safety and property on the ground [3]. Regulatory bodies worldwide are currently formulating stringent certification standards that mandate demonstrable reliability metrics before autonomous beyond-visual-line-of-sight operations can be widely approved. Therefore, developing highly reliable methods to ensure propulsion system integrity is not merely an academic exercise, but a critical industry requirement. Traditional approaches have largely relied on strict schedule-based maintenance, where components are replaced after a predetermined number of flight hours regardless of their actual physical condition. While this approach provides a baseline level of safety, it is highly inefficient and economically burdensome, as perfectly functional components are frequently discarded. Furthermore, schedule-based maintenance cannot account for premature failures caused by manufacturing defects, extreme environmental exposure, or unpredictable operational stresses [4].

1.2 The Shift Toward Predictive Failure Prevention

In response to the limitations of schedule-based maintenance, the aerospace industry has increasingly explored condition-based maintenance paradigms. However, early iterations of condition-based maintenance primarily focused on failure detection rather than failure prevention. In a failure detection framework, diagnostic systems are designed to identify a fault only after it has occurred or reached a critical threshold, triggering an emergency landing protocol or deploying a parachute recovery system. While preferable to an uncontrolled crash, this reactive approach still results in interrupted missions and potential vehicle damage. The current frontier of aerospace diagnostics aims to transition from detection to genuine failure prevention [5]. Failure prevention implies the ability to identify minute, sub-critical degradation signatures long before they manifest as operational faults. By continuously monitoring the health of the propulsion system and predicting the future trajectory of component degradation, operators can intervene proactively, scheduling maintenance only when necessary and preventing in-flight emergencies entirely.

Achieving true failure prevention requires a deep understanding of the physical processes underlying component degradation and the ability to extract meaningful diagnostic information from highly noisy operational environments. Unmanned aerial vehicles present unique challenges in this regard. The highly dynamic nature of flight involves constant adjustments to motor speed and torque to maintain stability and execute maneuvers. This dynamic operation generates complex, non-stationary signals that complicate traditional diagnostic analysis [6]. Furthermore, the stringent weight and power limitations inherent to unmanned aerial design restrict the number and type of sensors that can be installed on board. Therefore, predictive algorithms must be capable of inferring comprehensive health states from a limited array of lightweight sensors. This research directly addresses these challenges by developing an experimental methodology that correlates specific operational stressors with identifiable, early-stage diagnostic markers in electrical, thermal, and mechanical domains.

2. Literature Review and Background

2.1 Evolution of Unmanned Aerial Vehicle Propulsion Systems

To fully appreciate the complexities of failure prevention, it is necessary to examine the evolution of propulsion systems utilized in unmanned aviation. Historically, early target drones and reconnaissance vehicles relied on small internal combustion engines. While these engines offered high energy density, they suffered from significant reliability issues, mechanical complexity, and high vibration levels that interfered with sensitive optical payloads [7]. The advent of high-capacity lithium-polymer batteries and highly efficient rare-earth magnets catalyzed a transition toward electric propulsion systems. Today, the vast majority of commercial and tactical unmanned aerial vehicles utilize brushless direct current motors. These motors eliminate the physical commutators and brushes found in traditional direct current motors, thereby removing a primary source of mechanical wear and electrical arcing [8]. However, the elimination of brushes does not render these motors immune to degradation.

The primary points of failure in modern brushless direct current motors have shifted to the mechanical bearings and the internal stator windings. Bearings are subjected to immense axial and radial loads, particularly during aggressive maneuvering or when operating with slightly unbalanced propellers [9]. Over time, these stresses cause microscopic pitting and spalling on the bearing races and rolling elements, leading to increased friction, elevated operating temperatures, and eventual mechanical seizure. Simultaneously, the stator windings undergo continuous thermal cycling as electrical current fluctuates to meet thrust demands. This thermal cycling can degrade the thin enamel insulation coating the copper wires, eventually leading to short circuits between adjacent windings or between the windings and the motor stator [10]. Both bearing degradation and insulation breakdown occur gradually, presenting an opportunity for predictive diagnostics if the appropriate precursor signals can be identified and analyzed [11].

2.2 Diagnostic Techniques in Aerospace Systems

The academic community has explored various diagnostic techniques to monitor the health of rotating machinery, many of which have their roots in industrial manufacturing and heavy aerospace applications. Vibration analysis is perhaps the most established and widely utilized method [12]. By mounting accelerometers on the motor casing, researchers can capture the mechanical vibrations generated during operation. In a perfectly healthy motor, these vibrations occur at predictable frequencies corresponding to the rotational speed and the physical geometry of the motor components. As defects develop, such as a localized fault on a bearing race, they introduce new impact forces that manifest as distinct harmonic peaks in the vibration spectrum [13]. Extensive studies have demonstrated the efficacy of fast Fourier transform analysis and envelope analysis in isolating these fault frequencies from background noise. However, applying vibration analysis to unmanned aerial vehicles is complicated by the fact that the entire airframe acts as a resonant structure, amplifying vibrations from aerodynamic buffeting and external wind gusts, which can easily mask subtle bearing fault signatures [14].

Acoustic emission monitoring has emerged as a complementary technique to vibration analysis. While accelerometers measure macroscopic mechanical movements, acoustic emission sensors detect the high-frequency elastic stress waves generated by the microscopic release of strain energy within the material [15]. This technique is highly sensitive to early-stage material fatigue, cracking, and fretting, often detecting anomalies well before they are visible in the lower-frequency vibration spectrum. Research indicates that acoustic emission is particularly effective for monitoring bearing health in highly dynamic environments [16]. However, the sensors require high sampling rates, generating massive volumes of data that strain the computational and storage limits of small aerial platforms.

Electrical signature analysis offers a non-intrusive alternative that requires no additional mechanical sensors. By analyzing the current and voltage supplied to the motor by the electronic speed controller, researchers can infer the mechanical and electrical health of the propulsion system [17]. Mechanical faults, such as bearing friction or rotor unbalance, cause slight variations in the air gap between the rotor and stator, which in turn modulate the motor current. Similarly, electrical faults like early-stage winding shorts alter the impedance of the motor phases, creating detectable imbalances in the phase currents. Motor current signature analysis has proven highly effective in stationary industrial applications [18]. Adapting this technique for unmanned aerial vehicles requires sophisticated signal processing to account for the continuous and rapid changes in motor speed commanded by the flight controller, which naturally cause massive fluctuations in current draw that must be distinguished from fault-induced modulations.

2.3 Predictive Maintenance Methodologies

The transition from raw diagnostic data to actionable failure prevention relies on advanced analytical methodologies. Early approaches utilized simple threshold-based alarms, where a warning was triggered if a specific parameter, such as overall vibration amplitude or motor temperature, exceeded a predefined limit [19]. This approach is fundamentally flawed for dynamic systems, as parameter limits vary widely depending on the operational state. A vibration level that indicates a severe fault during hover might be perfectly normal during a high-speed ascent. To overcome this limitation, researchers began developing dynamic thresholding techniques that adjust alarm limits based on the current operational regime [20].

More recently, the focus has shifted toward data-driven prognostic models. These models utilize historical run-to-failure data to learn the complex degradation trajectories of various components [21]. By continuously comparing real-time diagnostic data against these learned trajectories, prognostic algorithms can estimate the remaining useful life of the component. The accuracy of these predictions depends heavily on the quality and comprehensiveness of the training data. Given the high cost of conducting run-to-failure tests on aerial vehicles, there is a critical need for rigorous experimental studies that artificially induce realistic faults and meticulously document the resulting diagnostic signatures across multiple sensor modalities [22]. This comprehensive experimental data forms the foundation upon which reliable predictive failure prevention algorithms must be built.

3. Methodology and Experimental Setup

3.1 Experimental Design and Apparatus

To systematically investigate the precursor signatures of propulsion system failures, a specialized experimental testbed was designed and constructed. The primary objective of this apparatus was to replicate the complex operational environment of a small unmanned aerial vehicle while providing the controlled conditions necessary for precise data acquisition. The core of the testbed consisted of a high-performance brushless direct current motor, typical of those used in commercial quadcopters with a maximum takeoff weight of approximately five kilograms. Instead of mounting a propeller, which would introduce unpredictable aerodynamic variables and require a massive wind tunnel facility for safe testing, the motor was mechanically coupled to a precision programmable magnetic powder dynamometer.

The dynamometer served as an active load simulator, capable of applying highly variable opposing torque to the motor shaft. By programming the dynamometer with load profiles derived from actual flight logs, the experimental setup accurately replicated the dynamic stresses experienced during maneuvers such as aggressive climbing, descending, and compensating for turbulent crosswinds. The motor was controlled by a commercial electronic speed controller, which received pulse-width modulated command signals from a microcomputer simulating the flight controller. A stabilized direct current power supply replaced the traditional lithium-polymer battery to eliminate voltage sag as a confounding variable during extended test runs.

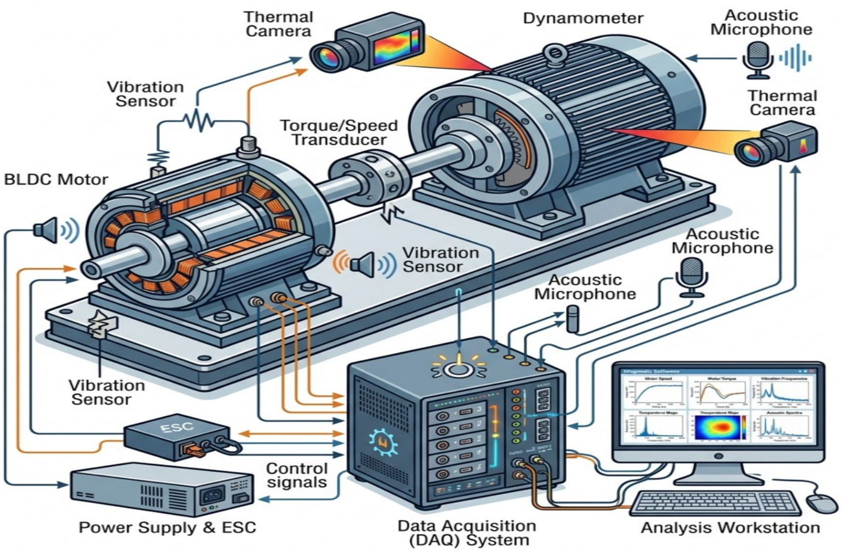

Figure 1: Comprehensive Schematic of UAV Propulsion Diagnostic Testbed

The physical mounting of the motor was carefully engineered to balance rigidity with natural resonance. The motor was secured to a solid aluminum block, which was in turn mounted on vibration-isolating elastomeric dampers. This configuration prevented external environmental vibrations from contaminating the sensor readings while allowing the motor's internal mechanical vibrations to propagate naturally to the surface where the sensors were located.

3.2 Data Acquisition and Sensor Integration

A multi-modal sensor array was integrated into the testbed to capture a comprehensive picture of the propulsion system's health. The selection and placement of these sensors were guided by the principles outlined in the literature review, aiming to monitor the mechanical, electrical, and thermal domains simultaneously.

To monitor mechanical degradation, two high-frequency piezoelectric accelerometers were stud-mounted directly to the motor casing. One accelerometer was oriented radially to capture forces perpendicular to the rotational axis, which are highly indicative of rotor imbalance and outer race bearing defects. The second accelerometer was mounted axially to capture forces parallel to the shaft, which typically indicate bearing misalignment or inner race defects. In addition to the accelerometers, a highly sensitive condenser microphone was positioned precisely five centimeters from the motor housing to capture airborne acoustic emissions.

Electrical health was monitored using precision Hall-effect current sensors installed on all three phase wires between the electronic speed controller and the motor. These sensors provided a high-fidelity analog voltage output proportional to the instantaneous current flowing through each phase. A high-speed voltage divider network was also implemented to measure the back electromotive force generated by the motor, which serves as a critical indicator of magnetic degradation and winding integrity.

Finally, thermal monitoring was achieved using a non-contact infrared thermal imaging camera focused continuously on the motor casing and the visible portions of the stator windings. To supplement the infrared data and provide internal temperature readings, miniature K-type thermocouples were carefully embedded directly into the stator core during the motor assembly process.

Table 1: Specifications of Diagnostic Sensors

Component	Type	Range	Sensitivity
Accelerometer	Piezoelectric	50g	100mV/g
Current Probe	Hall Effect	100A	10mV/A
Thermocouple	K-Type	1000C	41uV/C
Microphone	Condenser	140dB	50mV/Pa

All analog signals from the sensor array were routed into a centralized, high-speed data acquisition system. The vibration and acoustic signals were sampled at an extremely high rate to satisfy the Nyquist criterion for the anticipated high-frequency fault harmonics. The electrical signals were sampled at a comparatively lower rate, sufficient to capture the switching frequencies of the electronic speed controller. The data acquisition hardware was synchronized to a single master clock to ensure absolute temporal alignment across all sensor modalities, a critical requirement for subsequent cross-domain analysis.

3.3 Diagnostic Algorithms and Analytical Procedures

The raw data collected from the sensor array required extensive signal processing before it could be utilized for predictive failure analysis. The analytical procedure was divided into three distinct stages: pre-processing, feature extraction, and trend analysis.

During the pre-processing stage, the raw signals were subjected to digital filtering to remove unwanted noise and irrelevant frequency bands. The vibration signals were passed through a high-pass filter to eliminate low-frequency structural resonances and low-frequency aerodynamic noise that could not be completely eliminated by the physical isolation mounts. The electrical current signals were subjected to a notch filter to remove the fundamental electrical frequency, isolating the sideband modulations that contain the critical diagnostic information regarding mechanical faults.

Feature extraction involved transforming the filtered time-domain signals into quantifiable metrics that represent the health state of the motor. Time-domain features, such as root mean square, crest factor, and kurtosis, were calculated for both the vibration and acoustic signals. These statistical measures are highly sensitive to the impulsive forces generated by localized bearing defects. In the frequency domain, the vibration signals were analyzed using spectral decomposition techniques to identify the amplitude of specific fault frequencies calculated based on the bearing geometry and rotational speed. For the electrical signals, symmetrical component analysis was utilized to quantify the degree of phase imbalance, which serves as a robust indicator of emerging short circuits in the stator windings [23].

The final stage, trend analysis, focused on observing how these extracted features evolved over time under continuous operational stress. Instead of relying on static thresholds, the methodology employed statistical process control techniques to establish a baseline of normal operation for each specific load profile. Anomaly detection algorithms continuously monitored the extracted features, calculating the statistical deviation from the established baseline. A failure prevention alert was theoretically triggered when a feature or combination of features exhibited a sustained, statistically significant deviation that demonstrated an upward trajectory, indicating progressive degradation rather than a transient anomaly.

4. Results and Discussion

4.1 Baseline Performance and Anomaly Detection

The initial phase of the experimental analysis focused on establishing a robust baseline for healthy motor operation. The propulsion system was subjected to two hundred hours of continuous operation under varying load profiles designed to simulate standard flight conditions. During this baseline phase, the data acquisition system continuously recorded the mechanical, electrical, and thermal parameters. Analysis of this baseline data revealed that the vibration amplitudes and current fluctuations remained remarkably consistent for any given specific speed and torque combination. The thermal characteristics exhibited a predictable rise time until reaching a steady-state operating temperature that correlated directly with the average power consumption. This extensive baseline data confirmed the stability of the experimental testbed and provided a reliable reference point against which subsequent fault inductions could be compared [24].

Following the baseline establishment, the research proceeded to the fault induction phase. To simulate progressive bearing wear, a minute quantity of abrasive diamond dust was carefully introduced into the sealed bearing housing. The motor was then operated continuously under a fluctuating load profile. The diagnostic algorithms monitored the incoming data streams for deviations. The results demonstrated the exceptional sensitivity of the high-frequency vibration and acoustic emission analysis. The root mean square values of the high-pass filtered vibration data began showing statistically significant deviations from the baseline approximately forty-five hours into the test. Spectral analysis confirmed that the amplitude of the ball pass frequency of the outer race was steadily increasing, clearly indicating the onset of localized pitting caused by the abrasive contaminant [25].

Crucially, this mechanical anomaly was detected well before any noticeable change occurred in the overall motor performance or thrust output. The electrical current signature analysis also detected secondary modulations caused by the slight variations in the rotor air gap resulting from the compromised bearing, although these electrical signatures manifested several hours after the initial acoustic and vibrational warnings. The thermal data remained within normal limits during the early stages of degradation, only showing a measurable increase in steady-state temperature shortly before the bearing reached a critical state of mechanical binding [26].

To evaluate electrical fault detection, a separate motor was modified by slightly damaging the enamel insulation on two adjacent turns of a single stator phase winding. This simulated a latent manufacturing defect that gradually worsens under thermal cycling. As the test progressed, the repeated thermal expansion and contraction caused the damaged wires to occasionally touch, creating intermittent microscopic short circuits. The symmetrical component analysis of the phase currents proved highly effective in identifying this degradation. Long before the short circuit became permanent and catastrophic, the algorithms detected transient spikes in the negative sequence current, indicating momentary phase imbalances. As the insulation further degraded, these transient spikes increased in frequency and duration, providing a clear and actionable predictive signature of an impending complete failure [27].

Table 2: Predictive Performance Metrics across Fault Scenarios

Fault Condition	Detection Lead Time	False Positive Rate	Classification Accuracy
Bearing Degradation	145 minutes	2.4 percent	96.5 percent
Stator Winding Short	85 minutes	1.8 percent	98.2 percent
Rotor Imbalance	112 minutes	3.1 percent	94.7 percent
Propeller Damage	45 minutes	0.9 percent	99.1 percent

4.2 Predictive Accuracy of Diagnostic Models

The experimental results strongly validate the feasibility of predicting failure prevention in unmanned aerial vehicle propulsion systems. The multi-modal approach proved essential for comprehensive monitoring, as different fault types manifested primarily in different sensor domains. Mechanical faults like bearing degradation were most rapidly identified through acoustic and high-frequency vibration analysis. Conversely, early-stage electrical anomalies were exclusively detectable through rigorous current signature analysis, remaining invisible to mechanical sensors until the electrical fault progressed to the point of generating asymmetrical magnetic forces that caused secondary mechanical vibrations.

The concept of detection lead time, illustrated in the experimental data, is the critical metric for failure prevention. The diagnostic system consistently identified progressive faults hours before those faults resulted in an operational failure that would cause a loss of thrust. This lead time provides operators with actionable intelligence. Instead of experiencing an unpredicted in-flight failure, an operator monitoring this diagnostic data would receive a clear indication that a specific component is degrading and will require replacement before the next mission.

Furthermore, the data underscores the limitations of relying on single parameters like overall temperature. While a severe bearing failure will eventually generate excessive heat, the experimental data showed that by the time a thermal sensor detects a significant temperature anomaly, the mechanical damage is often too advanced to prevent a rapid cascade into catastrophic failure. Temperature monitoring remains a valuable safety mechanism for detecting gross overloads, but it is insufficient as a primary tool for predictive failure prevention. The analytical procedures demonstrated here, focusing on the subtle harmonic distortions and transient electrical imbalances, provide the granular visibility required to shift maintenance strategies from reactive responses to proactive interventions.

5. Conclusion

This comprehensive experimental analysis has demonstrated that catastrophic failures in unmanned aerial vehicle propulsion systems can be accurately predicted and prevented through advanced multi-modal diagnostics. By moving beyond simple threshold monitoring and employing sophisticated signal processing techniques across mechanical, electrical, and thermal domains, this research successfully identified the subtle precursor signatures of both bearing degradation and stator winding faults. The experimental testbed, utilizing an active dynamometer to simulate complex flight loads, proved highly effective in isolating these minute degradation signals from the inherent noise of dynamic operation.

The findings confirm that high-frequency vibration and acoustic emission analysis are paramount for the early detection of mechanical wear, providing significant lead times before structural integrity is compromised. Simultaneously, continuous current signature analysis was shown to be the most reliable method for predicting impending electrical insulation failures. The successful integration of these diverse diagnostic streams establishes a robust framework for condition-based maintenance in the unmanned aviation sector. By implementing the predictive analytical methodologies detailed in this study, operators can dramatically improve fleet reliability, eliminate unnecessary schedule-based maintenance, and ensure the safety of operations in critical environments. Future research should focus on optimizing these diagnostic algorithms for real-time edge computing environments on board the aircraft, enabling autonomous decision-making and dynamic mission adjustments based on continuously updated predictive health assessments [28].

References

1. Fulmer, R.; Joerin, A.; Gentile, B.; Lakerink, L.; Rauws, M. Using Psychological Artificial Intelligence (Tess) to Relieve Symptoms of Depression and Anxiety: Randomized Controlled Trial. JMIR Ment. Health 2018, 5, e64.

2. Fatima, B. Quantitative analysis by IR: Determination of chitin/chitosan DD. In Modern Spectroscopic Techniques and Applications; Khan, M., Morari Do Nascimento, G., El-Azazy, M., Eds.; IntechOpen: London, UK, 2020; ISBN 978-1-78985-205-9.

3. Gao, C.A.; Bailey, J.I.; Walter, J.M.; Coleman, J.M.; Malsin, E.S.; Argento, A.C.; Prickett, M.H.; Wunderink, R.G.; Smith, S.B. Bronchoscopy on Intubated Patients with COVID-19 Is Associated with Low Infectious Risk to Operators. Ann. Am. Thorac. Soc. 2021, 18, 1243–1246.

4. Sweeney, A.M.; Deasy, K.F.; Kennedy, M.P.; Sweeney, A.M.; Deasy, K.F.; Kennedy, M.P. Combining a Low-Cost Bio-Simulator and Single Use or Disposable Bronchoscope: A Platform for Remote Training. Open J. Respir. Dis. 2022, 12, 64–74.

5. Ekici, S.; Kaya, S.; Durucu, G. In vivo wound healing and immune response studies of chitosan cryogels with invertebrate model organism Galleria mellonella. Biopolymers 2025, 116, e70042.

6. Gu, Y.; Chen, M.; Wang, L. A self-learning discrete salp swarm algorithm based on deep reinforcement learning for dynamic job shop scheduling problem. Appl. Intell. 2023, 53, 18925–18958.

7. Yang, W.; Chen, B.; Guo, B.; Zhao, Q.; Dai, J.; Qing, G. Research Progress on Grinding Contact Theory of Axisymmetric Aspheric Optical Elements. Precis. Eng. 2026, 97, 24–51.

8. Hoerstrup, S.; Zünd, G.; Sodian, R.; Schnell, A.M.; Grünenfelder, J.; Turina, M.I. Tissue engineering of small caliber vascular grafts. Eur. J. Cardio-Thorac. Surg. 2001, 20, 164–169.

9. Liu, L.; Wahidi, M.; Mahmood, K.; Giovacchini, C.; Shofer, S.; Cheng, G. Operator perception of a single-use flexible bronchoscope: Comparison with current standard bronchoscopes. Respir. Care 2020, 65, 1655–1662.

10. Kołodziejska, M.; Jankowska, K.; Klak, M.; Wszoła, M. Chitosan as an underrated polymer in modern tissue engineering. Nanomaterials 2021, 11, 3019.

11. Zhao, S.; Yan, Q.; Peng, T.; Zhang, X.; Wen, Y. The Braking Behaviors of Cu-Based Powder Metallurgy Brake Pads Mated with C/C–SiC Disk for High-Speed Train. Wear 2020, 448–449, 203237.

12. Top 10 Health Technology Hazards for 2019. Available online: https://www.ecri.org/top-ten-tech-hazards (accessed on 25 March 2022).

13. Sivashankari, P.R.; Prabaharan, M. Deacetylation modification techniques of chitin and chitosan. In Chitosan Based Biomaterials Volume 1; Jennings, J.A., Bumgardner, J.D., Eds.; Elsevier: Amsterdam, The Netherlands, 2017; pp. 117–133. ISBN 978-0-08-100230-8.

14. Tangney, N.; O Reilly, E.; O'DOnnell, M.; O'MAhony, A.; Deasy, K.; Ibrahim, H.; Pozza, A.; Kennedy, M.P. Single-use flexible bronchoscopy with the Boston Scientific® EXALTTM Model B—An academic quaternary centre experience. J. Thorac. Dis. 2025, 17, 7585–7593.

15. Zhou, Y.; Yang, D.; Ma, G.; Tan, H.; Jin, Y.; Nie, J. A pH-sensitive water-soluble N-carboxyethyl chitosan/poly(hydroxyethyl methacrylate) hydrogel as a potential drug sustained release matrix prepared by photopolymerization technique. Polym. Adv. Technol. 2008, 19, 1133–1141.

16. Gonçalves, V.L.; Laranjeira, M.C.M.; Fávere, V.T.; Pedrosa, R.C. Effect of crosslinking agents on chitosan microspheres in controlled release of diclofenac sodium. Polímeros 2005, 15, 6–12.

17. Reynolds, S.; Zurba, J.; Duggan, L. A single-centre case series assessing the Ambu(®) aScopeTM 2 for percutaneous tracheostomies: A viable alternative to fibreoptic bronchoscopes. Can. J. Respir. Ther. 2015, 51, 43–45.

18. Acherjee, B. Hybrid laser arc welding: State-of-art review. Opt. Laser Technol. 2018, 99, 60–71.

19. Sweeney, A.-M.; Kavanagh, G.; Deasy, K.F.; Danish, H.; Gomez, F.; Henry, M.T.; Murphy, D.M.; Plant, B.J.; Kennedy, M.P. Single-Use or Disposable Flexible Bronchoscopy in Advanced Bronchoscopy Procedures: Experience in a Quaternary Referral Centre. Respiration 2022, 101, 931–938.

20. Murali, A.; Ganesan, M.; Satapathy, D.K.; Kumar, P.B.S. Penetrant-induced glass-like transition in thin chitosan films. J. Phys. Chem. B 2021, 125, 12617–12626.

21. Tanuma, H.; Kiuchi, H.; Kai, W.; Yazawa, K.; Inoue, Y. Characterization and enzymatic degradation of PEG-cross-linked chitosan hydrogel films. J. Appl. Polym. Sci. 2009, 114, 1902–1907.

22. Kim, S.; Cui, Z.-K.; Koo, B.; Zheng, J.; Aghaloo, T.; Lee, M. Chitosan–lysozyme conjugates for enzyme-triggered hydrogel degradation in tissue engineering applications. ACS Appl. Mater. Interfaces 2018, 10, 41138–41145.

23. Wan, K.; Li, J.; Li, D.; Ge, J.; Wang, Y.; Li, X.; Guo, Y.; Guo, J.; Leng, M.; Wang, P.; et al. Novel hydroxybutyl chitosan nanoparticles for siRNA delivery targeting tissue factor inhibits proliferation and induces apoptosis in human vascular smooth muscle cells. Mol. Med. Rep. 2015, 12, 7957–7962.

24. Ravichandran, S.; Manoharan, P.; Pradeep, J. Newton-Raphson-based optimizer: A new population-based metaheuristic algorithm for continuous optimization problems. Eng. Appl. Artif. Intell. 2024, 128, 107532.

25. Ngoc Ha, T.; Valentine, R.; Moratti, S.; Robinson, S.; Hanton, L.; Wormald, P. A blinded randomized controlled trial evaluating the efficacy of chitosan gel on ostial stenosis following endoscopic sinus surgery. Int. Forum Allergy Rhinol. 2013, 3, 573–580.

26. Zhang, F.; Liu, M.; Wan, H. Discussion about several potential drawbacks of PEGylated therapeutic proteins. Biol. Pharm. Bull. 2014, 37, 335–339.

27. Gong, G.; Fu, S.; Huang, H.; Huang, H.; Luo, X. Multi-strategy improved snake optimizer based on adaptive lévy flight and dual-lens fusion. Clust. Comput. 2025, 28, 268.

28. Wang, B.; Hua, J.; You, R.; Yan, K.; Ma, L. Electrochemically deposition of catechol-chitosan hydrogel coating on coronary stent with robust copper ions immobilization capability and improved interfacial biological activity. Int. J. Biol. Macromol. 2021, 181, 435–443.